Tuning nano electric field to affect restrictive membrane area on localized single cell nano-electroporation

Tuhin Subhra Santra, Pen-Cheng Wang, Hwan-You Chang, and Fan-Gang Tseng

Citation: Applied Physics Letters **103**, 233701 (2013); doi: 10.1063/1.4833535
View online: http://dx.doi.org/10.1063/1.4833535
View Table of Contents: http://scitation.aip.org/content/aip/journal/apl/103/23?ver=pdfcov
Published by the AIP Publishing

Tuning nano electric field to affect restrictive membrane area on localized single cell nano-electroporation

Tuhin Subhra Santra,[1] Pen-Cheng Wang,[2] Hwan-You Chang,[3] and Fan-Gang Tseng[1,2,3,4]
[1]*Institute of Nano Engineering and Microsystems, National Tsing Hua University, Hsinchu City, Taiwan*
[2]*Department of Engineering and System Science, National Tsing Hua University, Hsinchu City, Taiwan*
[3]*Department of Medical Science, National Tsing Hua University, Hsinchu City, Taiwan*
[4]*Division of Mechanics, Research Center for Applied Sciences, Academia Sinica, Taipei, Taiwan*

(Received 21 August 2013; accepted 31 October 2013; published online 2 December 2013)

Interaction of electric field with biological cells is an important phenomenon for field induced drug delivery system. We demonstrate a selective and localized single cell nano-electroporation (LSCNEP) by applying an intense electric field on a submicron region of the single cell membrane, which can effectively allow high efficient molecular delivery but low cell damage. The delivery rate is controlled by adjusting transmembrane potential and manipulating membrane status. Thermal and ionic influences are deteriorated from the cell membrane by dielectric passivation. Either reversible or irreversible by LSCNEP can fully controlled with potential applications in medical diagnostics and biological studies. © *2013 AIP Publishing LLC* [http://dx.doi.org/10.1063/1.4833535]

Electroporation or electropermeabilization is a technique where high electric field is applied in between two large electrodes to form permeable transient nanopores on the cell membrane, which allow foreign species such as DNA, RNA, oligonucleotides, dyes, protein, and gene to enter from outside to inside of the cell with complete membrane resealing, which is known as reversible electroporation, or allow intracellular compound from inside to the outside of the cell, known as irreversible electroporation with complete membrane rupture.[1–4] Due to application of high external electric field, cell membrane increases their conductivity and permittivity, where these values are different from outside to inside of the cell. This potential difference across the cell membrane is known as transmembrane potential (TMP), which can be expressed for cell in spherical shape as[5]

$$\Delta TMP = 1.5\ r_{cell}\ E\cos(\theta)\ , \tag{1}$$

where E is the external electric field, r_{cell} is the cell radius, and θ is the polar angle with respect to the direction of the field. The value of the transmembrane potential is approximately 0.2 V–1.0 V mostly from the experiment of bulk and single cell electroporation.[6,7] Once the cell membrane potential achieves this certain threshold value due to external applied voltage, pores will form on the cellular membrane, and it can reseal after withdrawing the external field. The size and density of the pores depend upon external field strength, pulse duration, and number of pulses. For very high external voltage, membrane threshold value can easily exceed this value (0.2 V–1.0 V) resulting in cell lysis or known as irreversible electroporation. Recently single cell membrane nano-electroporation in a localized region has attracted much attention due to high transfection rate and high cell viability.[8–12] However the effect of highly intensive electric field with the variation of TMP in a local region of the single cell membrane was not well studied previously. Higher electric field effects the whole single cell (familiar as single cell electroporation (SCEP)) to cause cell lysis easily. In this paper, we demonstrate localized single cell nano-electroporation (LSCNEP) with nano-electrodes, where an intense electric field focused in a very local region of single cell membrane can greatly enhance electroporation condition and allow high cell viability. The size of affected membrane area in the local region of a single cell can be well controlled by adjusting different external applied voltages. As a result, the destructive and nondestructive localized single cell membrane nano-electroporation can easily be manipulated with the variation of affected TMP area, where higher delivery rate is provided due to higher affected membrane area. Beyond certain voltage, cell lysis happens, where TMP (~1 V) exceeds cell membrane threshold values.[7] Very high voltage induces larger affected membrane area with one to several large pores, resulting in membrane rupture and finally cell death.

For LSCNEP, the schematic representation of this device is shown in Fig. 1, where electric field is applied intensively at a local region of the single cell membrane. For simulation of this device, COMSOL Multiphysics (version 3.5, Sweden) software was used to simulate the electric field and resistive heat effects on the membrane surface. Fig. 2(a) shows the electric field distribution with affected cell membrane area, where electric field is limited in between a 500 nm gap and 8 V applied voltage. We assume that human caucasian gastric adenocarcinoma (AGS) cell membrane has little bending within 500 nm gap. Fig. 2(b) shows resistive heat effects on the membrane surface, where we consider

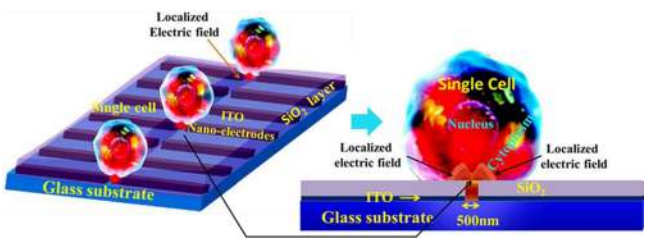

FIG. 1. Schematic representation of LSCMEP chip, where an intense electric field affects a small region of the cell membrane to permeate drug from outside to inside of the cell.

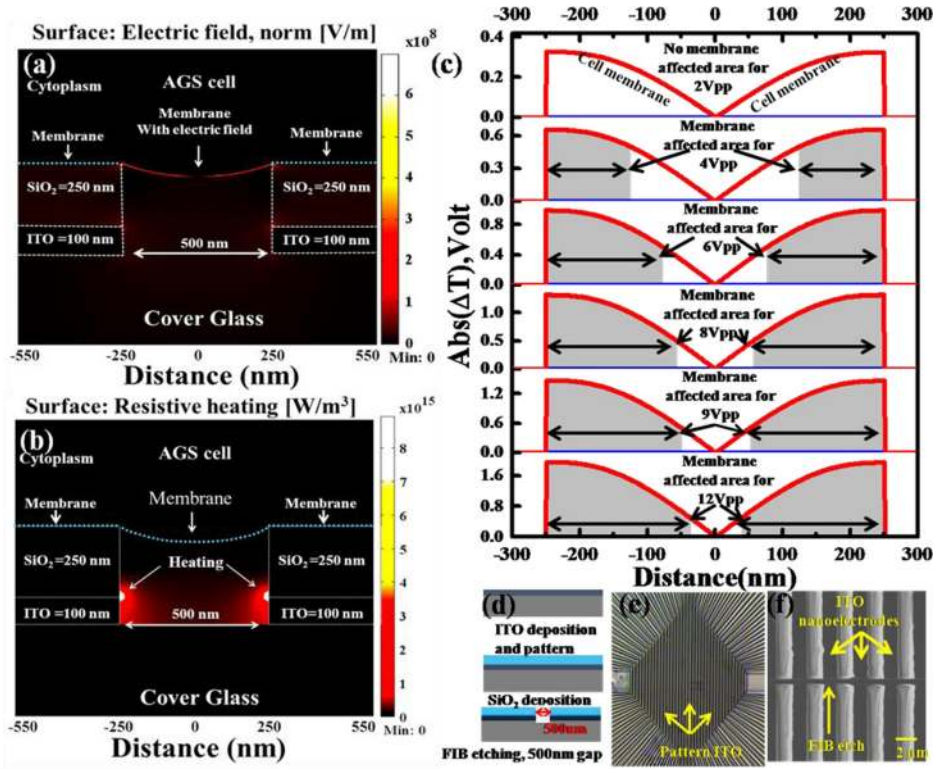

FIG. 2. COMSOL Multiphysics simulation for LSCMEP process. (a) Electric field distribution on localized single cell membrane surface, where field intense maximum 3×10^8 V/m at the edge of the nano-electrodes and the field was absent at the middle between two nano-electrodes at 8Vpp voltage. (b) Resistive heating effect which was maximum at the edge of the nano-electrodes, and it cannot reach to the cell membrane due to 250 nm SiO_2 passivation layer. (c) Transmembrane potential distribution in between two nano-electrodes (for 2Vpp to 12Vpp). Higher applied voltage providing higher transmembrane potential area (shaded region is considered from 0.653 V because molecular delivery started from this values) causes higher affected membrane area. (d) Fabrication process of LSCMEP chip. (e) Optical microscope image of patterned ITO lines after wet chemical etching. (f) SEM image of focused ion beam (FIB) etched ITO nano-electrodes. 500 nm gap between two ITO nano-electrodes.

250 nm SiO_2 layer as an electric field passivation layer. Simulation result shows that heat is generated much more on the edge of the two nano-electrodes, retaining a 250 nm distance from the cell membrane, which not only avoids direct heating on the cell membrane surface but also minimizes the effect to generate hydroxyl and hydrogen ions during nano-electroporation process.[13,14] To calculate TMP, we consider SiO_2 layer as well as extracellular matrix such as protein layer (10 nm–15 nm) which formed in between chip surface and cell membrane.[10,15,16] As a result, we simulate TMP with 265 nm layer from the nano-electrode surface. Fig. 2(c) shows the TMP distribution with affected membrane area (shaded region) for localized single cell nano-electroporation in 500 nm gap with 2Vpp–12Vpp external applied voltages. This simulation result shows that the TMP is higher at the edge of the nano-electrodes and it reduces continuously in the middle of the nano-electrodes gap (almost zero). According to experimental results (Figs. 4 and 5, discussed later), molecular delivery with reversible electroporation started approximately at 4Vpp, and irreversible electroporation (cell lysis) was observed approximately at 9Vpp applied voltage. At 4Vpp, the TMP value was 0.604 V; as a result, affected membrane area (shaded region) was calculated with a minimum 0.604 V consideration. For

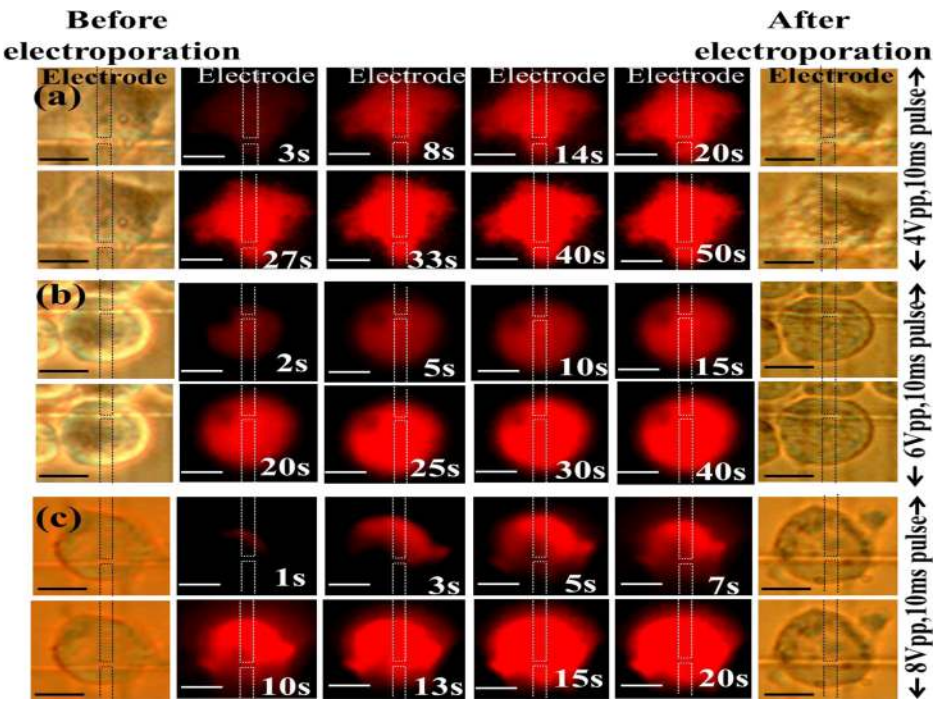

FIG. 3. Time dependent cell survival fluoresce image and optical image (before/after electroporation) of AGS cell where intensity increases continuously with time (a) 4Vpp, 10 ms (3 pulses), (b) 6Vpp, 10 ms (3 pulses), (c) 8Vpp, 10 ms (3 pulses). Scale bar 5 μm.

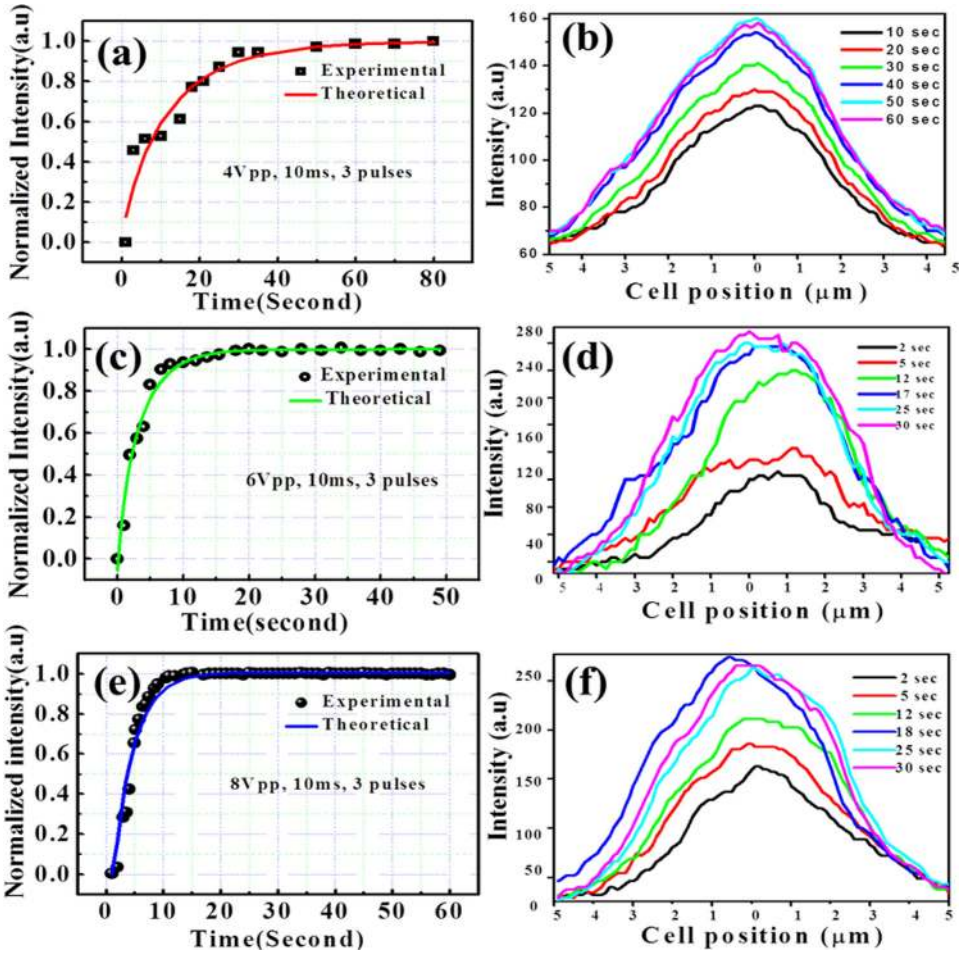

FIG. 4. Correlation between experimental, theoretical diffusion model and intensity distribution with different cell positions. (a) Theoretical and experimental correlation of diffusion model for 4Vpp, 10 ms (3 pulses). (b) Intensity distribution in a single cell with different times (intensity captured from middle of the cell with line profile function using Image pro plus software). At longer times, intensity curves overlap with each other, which suggested that intensity saturates at longer times (4Vpp, 10 ms pulse (three pulses). (c), (d) Correlation of theoretical and experimental diffusion model and intensity distribution with different times for 6Vpp, 10 ms (3 pulses) and (e), (f) for 8Vpp, 10 ms (3 pulses).

2Vpp applied voltage, there was no such molecular delivery (for 0.302 V TMP) from our experiment. At 4Vpp (Fig. 2(c), shaded region), the affected membrane area near in each nano-electrode edge was ($2\,\mu m \times 125$ nm, where $2\,\mu m$ was electrode width). As a result, total affected (both nano-electrode edge) membrane area was [($2\,\mu m \times 125$ nm) + ($2\,\mu m \times 125$ nm)] within 500 nm gap between two nano-electrodes. The total affected membrane area was larger [($2\,\mu m \times 215$ nm) + ($2\,\mu m \times 215$ nm)] in Fig. 2(c)] at 12Vpp applied voltage compared to lower applied voltage (4Vpp). The detail of affected membrane area has shown in Table I. In Figure 2(c), each position of the membrane has different TMP values resulting in the formation of different density of pores in each area of the membrane.[12] Also, the density of pores should be larger on the edge of the nano-electrodes because of high TMP values.

TABLE I. Parameters for different applied voltages including diffusion coefficient, deviation factor, time constant, affected membrane area within 500 nm gap [($2\,\mu m$ + affected area of one electrode edge) + ($2\,\mu m$ + affected area of another electrode edge)], and transmembrane potential with 265 nm passivation layer consideration.

Voltage (V)	D (m^2/s)	A	τ (sec)	Membrane affected area with in 500 nm in each edge of nano-electrode	Transmembrane potential (V)
2					0.302
4	1.7×10^{-13}	1.28	14.4 ± 3.2	125 nm	0.604
6	6.5×10^{-13}	1.38	3.9 ± 0.3	175 nm	0.907
8	7.0×10^{-13}	2.28	3.6 ± 0.2	193 nm	1.209
9				200 nm	1.360
12				215 nm	1.814

The fabrication process detail has been described in Ref. 17. Fig. 2(d) shows the fabrication process step of the LSCNEP chip while the patterned Indium Tin Oxide (ITO) lines are shown in Fig. 2(e). Fig. 2(f) shows 500 nm gap between two nano-electrodes. ($2\,\mu m$ width and 90 nm thickness as consider as nano-electrode, because one dimension is less than 100 nm).

To demonstrate LSCNEP process, we have used AGS cancer cell line. A detail of cell culture has been provided in Ref. 17. Initially, cells were randomly attached onto the chip surface, but those cells sitting in between top of the two nano-electrodes (see Fig. 1) were selected for the LSCNEP experiment.[17] Since the gap between two nano-electrodes was 500 nm, resulting in an intensive electric field effect, only a small fraction of the three dimensional volume of the single cell membrane induces permeable membrane nanopores whereas the other area of the cell membrane was remaining unaffected. For our experiment, we have used function generator to apply 1Vpp–12Vpp single positive square wave with 10 ms pulse (3 pulses together) in each case. However we cannot found any molecular delivery below 4Vpp, 10 ms pulse. At lower voltage, TMP (at 2Vpp, TMP was 0.302 V, see Table I) cannot reach cell membrane threshold to promote long-lived pores. However, short-lived pores can be generated, but it cannot transport molecules.[18] Moreover, lower voltage affects less membrane area with

lower energy which might be unable to create permeable nanopores. In our experiment, we used molecular dye as propidium iodide (PI), which cannot enter continuously into live cell without membrane rupture, and this dye was introduced into the electroporation chamber, just prior to electrical pulse application. Fig. 3 shows cell survival fluorescence image of AGS cell with different time durations. We have applied 4Vpp [Fig. 3(a)), 6Vpp (Fig. 3(b)), and 8Vpp (Fig. 3(c)] with 10 ms pulse (three pulses together), where intensity increases continuously with increase of time. However, for higher voltage (8 V), intensity was much higher and saturation took shorter time compared with lower voltage (4 V). In Figs. 3(a)–3(c) we have plotted normalized intensity with different time durations and have correlated this experimental data with theoretical diffusion model to evaluate diffusion coefficient, deviation factor, and time constant (Table I, Ref. 17).

Figs. 4(a) and 4(b) show normalized intensity distribution with different times and corresponding intensity profile with cell positions (intensity is higher at middle of the cell and captured it with line profile function by Image pro plus software) for 4Vpp with 10 ms pulse, whereas Figs. 4(c) and 4(d) and Figs. 4(e) and 4(f) show the normalized intensity and intensity profile for 6Vpp and 8Vpp with 10 ms pulse application. In Figs. 4(a), 4(c), and 4(e), we correlate experimental data with theoretical model. After application of pulses (4Vpp, 10 ms in Fig. 4(a)), intensity increases slowly with different times from 0 to 40 s, indicating that PI dye diffuses slowly into the cell or dye has tendency to enter inside cell, but due to insufficient nanopores area, dye cannot enter freely inside the cell. Also, for lower voltage, the density of pores with affected membrane area ($2\,\mu m \times 125$ nm in front of in each electrode) was smaller. It might happen that the maximum pores with lager size only open at the edge of the nano-electrodes (because TMP values were higher at the edge of the nano-electrodes and reduce continuously in the middle of the two nano-electrodes, see Fig. 2(c)), and in the remaining area, the pores were not open at this voltage. Thus intensity saturation took longer time. After 40 s, the intensity was almost saturated, indicating that the concentration gradient across the cell membrane becomes zero. There is also another possibility that nanopores reseal after this time and dye cannot enter inside the single cell. According to theoretical calculation, the diffusion coefficient and deviation factor were approximately 1.7×10^{-13} m^2/s and 1.28, which were lower when compared to the higher voltages [see Table I], suggesting slower PI dye delivery inside single cell. The time constant for 4Vpp applied voltage was 14.4 ± 3.2, indicating slower dye delivery inside single cell. In Fig. 4(b), intensity increases as time increases and was saturated at longer time (nearly 40 s, intensity profiles overlap with each other, suggesting intensity saturation), followed by diffusion mechanism.

In Fig. 4(c), the intensity profile is due to application of 6Vpp 10 ms pulse, where intensity saturates with less time compared to 4Vpp, 10 ms pulse. For higher applied voltage, energy is increased to form more density of pores with larger affected membrane area ($2\,\mu m \times 175$ nm, in front of each nano-electrode (see Fig. 2(c) and Table I)).[19–21] However, pore openings areas were the same as 4Vpp because of same duration of pulses.[12,19] Because of increase of affected membrane area with higher density of pores, PI dye diffuses very fast inside the single cell, and it saturates after 15 s–20 s. Saturation indicated that concentration gradient was similar between inside or outside of the cell. The pores were long-lived, and they can open for seconds to minutes and then reseal.[12,18] However, resealing time of the pores strongly depends upon temperature and adenosine triphosphate (ATP) dependent biological process.[18] In our device SiO_2 passivation layer was deposited on the top of the nano-electrodes, which can effectively avoid the temperature influence onto the cell membrane directly. As a result, membrane might be resealed within several seconds for our experiment. In Fig. 4(d), intensity increases as time increased, and it was saturated at 20 s, where intensity profiles overlap with each other, indicating that holes are resealed at higher times or concentration gradient becomes zero across the cell membrane.

Fig. 4(e) shows the intensity profile for 8Vpp, 10 ms pulse, where intensity saturates at very less time, and Fig. 4(f) shows intensity distribution with different times. To apply very high voltage, higher energy was available to form the long-lived pores, and the stability of these pores was higher due to much more free energy from large conductive pores.[22] As a result, affected membrane area ($2\,\mu m \times 193$ nm, in each nano-electrode edge) was increased with much larger density of pores in comparison with lower voltages (see Table I), resulting in very fast molecular delivery into the cell.[9,12] Thus saturation took very short time (15 s). From Table I, the TMP at this voltage was 1.209 V which almost exceeds membrane threshold values.[6,7] Thus at (8Vpp), very high density of pores are suggested to connect with each other to form several larger pores at the edge of each nano-electrode, resulting in very fast molecular delivery. The diffusion coefficient and deviation factor were 7.0×10^{-13} m^2/s and 2.28, suggesting that the affected membrane area for diffusion increases with increase of applied voltage (see Table I). The time constant for 8Vpp voltage was 3.6 ± 0.2, which was lower when compared to 4Vpp and 6Vpp voltage, suggesting very fast molecular delivery into the cell. Beyond 8Vpp pulses, we found irreversible electroporation mechanism.

For 9Vpp, 10 ms pulse (3 pulses), irreversible electroporation was observed. At this higher voltage, cell membrane affected area was much larger ($2\,\mu m \times 200$ nm, in front of each nano-electrode) due to very high energy, resulting in larger density of pores formation, and each pore might be connected together to form only one pore or several larger area of pores which unable to reseal again after withdrawing the pulse. As a result, membrane deforms permanently. For very high energy, large deformation of the cell membrane leads to the high stability of pores opening. Thus irreversible electroporation occurred beyond 8Vpp voltage. The TMP values was much higher (1.36 V) which exceeds much more in comparison with cell membrane threshold values (0.2 V–1.0 V), and beyond these values, irreversible electroporation occurred due to membrane rupture.[7] At 12Vpp, the affected membrane area was ($2\,\mu m \times 215$ nm) very high with high TMP (1.814 V), resulting in complete membrane rapture in between 500 nm gap, and finally cell death. From Table I, it is clear that higher voltage provides very high affected membrane area, high transmembrane potential, high diffusion coefficient, and high deviation factor compared to lower voltage which results in fast molecular delivery with

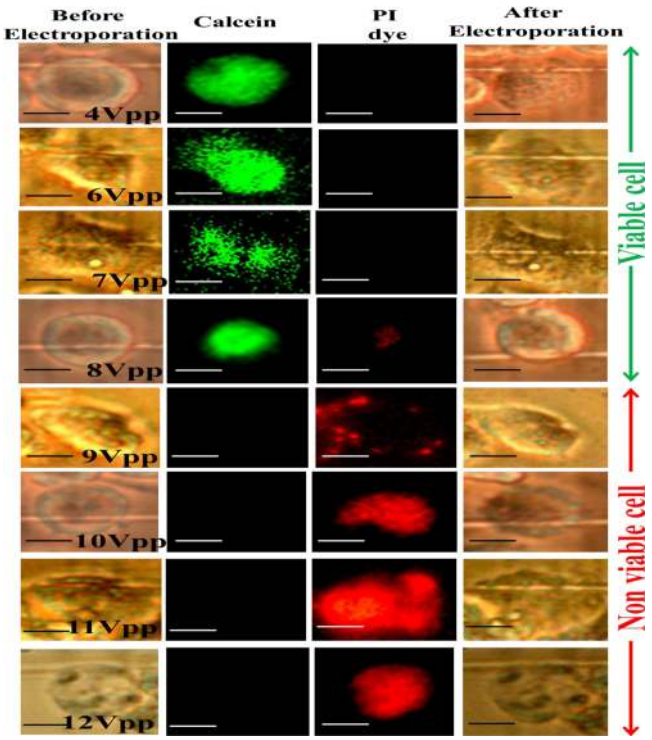

FIG. 5. Reversible and irreversible electroporation with different applied voltages. Reversible electroporation started from 4Vpp to 8Vpp, and irreversible electroporation was observed from 9Vpp to 12Vpp external applied voltages. Scale bar 5 μm.

less time constant. Thus to control external applied voltage, it is possible to optimize affected membrane area, resulting in reversible and irreversible electroporation. In our study, under TMP [0.2 V TMP + 0.102 V = 0.302 V] for 2Vpp not provided any molecular delivery due to lower affected membrane area (no shadow region in Fig. 2(c)), but TMP (0.2 V TMP + 0.404 V = 0.604 V) for 4Vpp provided initial molecular delivery within 2 μm × 125 nm affected membrane area in front of each nano-electrode. On the contrary, over TMP (1 V TMP + 0.209 V = 1.209 V) for 8Vpp promote very fast molecular delivery with 2 μm × 193 nm membrane area in each nano-electrode edge. Exceedingly, very high over TMP (1 V TMP + 0.360 V = 1.360 V) for 9Vpp provided larger affected membrane area [2 μm × 215 nm, at one edge of the nano-electrodes, see Fig. 2(c)], resulting in complete cell lysis (irreversible electroporation).

Fig. 5 shows the cell viability and cell shape, before and after electroporation experiment. To test the cell viability after electroporation as well as electroporation induced cell death or apoptosis, we have used cell permeable calcein for live cell and PI dye for dead cell, stained simultaneously. After electroporation without any dye introduction into the chip, we incubated cells on this electroporated chip for 30–40 min in an incubator. Then we introduced calcein AM into the chip and waited for few minutes. If the cell provided green fluorescence, image indicated as cell is live. However, to test whether the cell is dead or not, after viability test by calcein, we introduced PI dye into the same chip again. If it provides red fluorescence image, it is the indication that the cell is dead. As in Fig. 5, the cells are viable for 4 V, 6 V, 7 V, and 8 V (calcein hydrolysis inside the live cell) whereas cells are dead for 9 V, 10 V, 11 V, and 12 V applied voltage (PI dye bind with nucleus of dead cell[23]). The cell viability rate was almost 80% after one day at 8 V external applied voltage. However viability was increases up to 95%, when the external voltage was 4Vpp.

In summary, we present localized single cell nano-electroporation with reversible as well as irreversible electroporation mechanism with different TMP values. Lower TMP values (0.2 V TMP + 0.404 V = 0.606 V) provide less affected membrane area with lower density of pores on the cell membrane, resulting in slow delivery of molecules into the single cell. However, extremely high electric field promotes very high affected membrane area with larger density of pores, resulting irreversible electroporation [over TMP (1 V) + 0.209 V = 1.209 V]. This device can perform reversible and irreversible electroporation with controllable affected membrane area by adjusting external applied voltages, which is potentially beneficial for biological cell studies and therapeutic applications.

The authors greatly appreciate the financial support from National Science Council (NSC) of Taiwan ROC through Biomedical Engineering Program (NSC-101-2221-E-007-032-MY3) and National Nanotechnology and Nanoscience Program (NSC-101-2120-M-007-001).

[1]E. Neumann, M.-S. Ridder, Y. Wang, and P. H. Hofschneider, EMBO J. **1**(7), 841–845 (1982).
[2]T. Tsong, Biophysics. J. **60**(2), 297–306 (1991).
[3]Y.-C. Lin and M.-Y. Huang, J. Micromech. Microeng. **11**, 542–547 (2001).
[4]Y. S. Shin, K. Cho, J. K. Kim, S. H. Lim, C. H. Park, K. B. Lee, Y. Park, C. Chung, D.-C. Han, and J. K. Chang, Anal. Chem. **76**, 7045–7052 (2004).
[5]C. Grosse and H. P. Schwan, Biophys. J. **63**, 1632–1642 (1992).
[6]U. Zimmermann, Biochim. Biophys. Acta **694**(3), 222–227 (1982).
[7]B. Rubinsky, Irreversible Electroporation (Springer, Heidelberg, 2009).
[8]S. Mavahed and D. Li, Microfluid. Nanofluid. **10**, 703–734 (2011).
[9]P. E. Boukany, A. Morss, W.-C. Liao, B. Henslee, H. C. Jung, X. Zhang, B. Yu, X. Wng, Y. Wu, L. Li, K. Gao, X. Hu, X. Zhao, O. Hemminger, W. Lu, G. P. Lafyatis, and L. J. Le, Nat. Nanotechnol. **6**, 747–754 (2011).
[10]N. Jokilaakso, E. Salm, A. Chen, L. Millet, C. D. Guevara, B. Dorvel, B. Reddy, Jr., A. E. Karlstrom, Y. Chen, H. Ji, Y. Chen, R. Sooryakumar, and R. Bashir, Lab Chip **13**, 336–339 (2013).
[11]D. Nawarathna, K. Unal, and H. K. Wickramasinghe, Appl. Phys. Lett. **93**, 153111 (2008).
[12]S.-C. Chen, T. S. Santra, C.-J. Chang, T.-J. Chen, P.-C. Wang, and F.-G. Tseng, Biomed. Microdevices **14**(5), 811–817 (2012).
[13]W. G. Lee, H. Bang, H. Yun, J. Min, C. Chung, J. K. Chang, and D. C. Han, Lab Chip **8**, 224–226 (2008).
[14]J. A. Kim, K. Cho, M. S. Shin, W. G. Lee, N. Jung, C. Chung, and J. K. Chang, Biosens. Bioelectron. **23**, 1353–1360 (2008).
[15]B. Alberts, A. Johnson, J. Lewis, M. Raff, K. Roberts, and P. Walter, *Molecular Biology of the Cell* (Garland Science, New York, NY, 2002).
[16]M. M. Browne, G. V. Lubarsky, M. R. Davidson, and R. H. Bradley, Surf. Sci. **553**, 155–167 (2004).
[17]See supplementary material at http://dx.doi.org/10.1063/1.4833535 for X-Ray Diffraction (XED) results, light transparent by UV-VIS spectroscopy, diffusion coefficient, deviation factor calculation and AGS cell image on top of the chip, etc.
[18]M. Pavlin, V. Leben, and D. Miklavcic, Biochem. Biophys. Acta **1770**, 12–23 (2007).
[19]B. Gabriel and J. Tissie, Biophys. J. **73**, 2630–2637 (1997).
[20]J. A. Lundquist, F. Sahlin, M. A. Aberg, A. Strimberg, P. S. Eriksson, and O. Orwar, Proc. Natl. Acad. Sci. U.S.A. **95**, 10356–10360 (1998).
[21]E. Takle, R. D. Astumian, and P. B. Chock, Biochem. Biophys. Res. Commun. **172**, 282–287 (1990).
[22]R. M. Schmid, H. Weidenbach, G. F. Draenert, S. Liptay, H. Lührs, and G. Adler, Gut **41**, 549–556 (1997).
[23]M. P. Rols and J. Teissie, Biophys. J. **75**, 1415–1423 (1998).